17th International Conference on Greenhouse Gas Control Technologies, GHGT-17

20th -24th October 2024 Calgary, Canada

Screening CO_2 storage potential of petroleum reservoirs on Norwegian Continental Shelf

Alexey Khrulenko [a]*, Trine Mykkeltvedt [a], Sarah E. Gasda [a,b]

[a] *NORCE Norwegian Research Center, Nygårdsgaten 112, 5008 Bergen, Norway*

[b] *University of Bergen, Allégaten 41, 5007 Bergen, Norway*

Abstract

This study aims to assess the CO_2 storage potential of petroleum fields on the Norwegian Continental Shelf (NCS). Publicly available data about the reservoirs were gathered, processed, and enriched to fill data gaps and enable further analysis. A set of indicators was then proposed to infer CO_2 storage capacity, injectivity, and other relevant parameters through the available data and production history, in particular. The original and enriched data, along with the derived indicators, were compiled into a database that covers 134 Norwegian fields. The total storage capacity indicator was estimated at 18 Gt with 64% in the ten largest fields and 69% attributed to gas production.

While the proposed approach and its results do not resolve all uncertainties, they allow for screening, refining possible options, identifying key areas for further detailed studies, and consistently comparing candidate reservoirs. The suggested methodology was illustrated by two case studies.

The data and codes are made available at *https://github.com/cssr-tools/SubCSeT*. Additionally, a web application for visualization and screening is available at *https://subcset-35e143428f88.herokuapp.com*.

Keywords: CO_2 storage; screening; ranking; petroleum fields; Norway; Norwegian Continental Shelf

draft

1. Introduction

To fulfil Europe's CO_2 abatement objectives in the coming years, substantial new initiatives are needed to secure sufficient and economical CO_2 storage capacity. Repurposing depleted petroleum fields can play a key role in achieving this goal. Although there are several CO_2 storage projects on the NCS targeting saline aquifers, relatively few studies have considered pure CO_2 storage (i.e., without an enhanced oil recovery component) in depleted petroleum fields. Meanwhile, many of them may become ideal candidates for CO_2 storage, as they often possess ample pore space, good flowing properties, and caprocks that have securely contained hydrocarbons for many thousands of years. To date, around 130 petroleum fields on the Norwegian Continental Shelf (NCS) have been approved for production and, as of December 31, 2023, 55% of the resources have been produced ([1], figure 4.3) which implies large released pore volumes that can be reused. Given the increasing demand for CO_2 storage, and presence of abandoned or soon-to-be-abandoned fields near existing infrastructure, we believe that their potential is likely to be utilized in the future. As in the case of natural gas storage in the USA, where depleted petroleum reservoirs account for 78.2% of total storage capacity, compared to 14.8% in aquifers and 7% in caverns [2].

* Corresponding author. Tel.: +47 51 87 52 74, *E-mail address:* alkh@norceresearch.no

This study presents an approach for screening petroleum fields on the NCS for CO_2 storage based mainly on well and reservoir data made publicly available by the Norwegian Offshore Directorate (NOD) [3,4]. The second part presents data processing, enrichment and use to assess parameters important for CO_2 storage. The third part demonstrates the methodology through case studies. The paper concludes with discussion on applicability and limitations of the proposed approach and suggests ways forward.

The described screening approach was implemented in a web application openly available at *https://subcset-35e143428f88.herokuapp.com*. The data and codes are available at *https://github.com/cssr-tools/SubCSeT*.

2. Methodology

2.1. Data sources

The main idea of our approach is to use publicly available reservoir data and production history to derive certain *indicators* relevant for CO_2 storage. A brief overview of data sources, data flows and resulting indicators is presented in Fig. 1. The main data sources used in our study are:

- The FactPages of the Norwegian Offshore Directorate [3]:
  - field descriptions: main producing groups and formations, coordinates, lithology,
  - field in-place and recoverable volumes,
  - field production profiles,
  - wellbore data: final depth (SSTVD), temperature, type, completion date.
- DISKOS (public portal) [4]:
  - field production and injection rates,
  - well production and injection rates.
- publications:
  - initial pressures, temperatures, depths

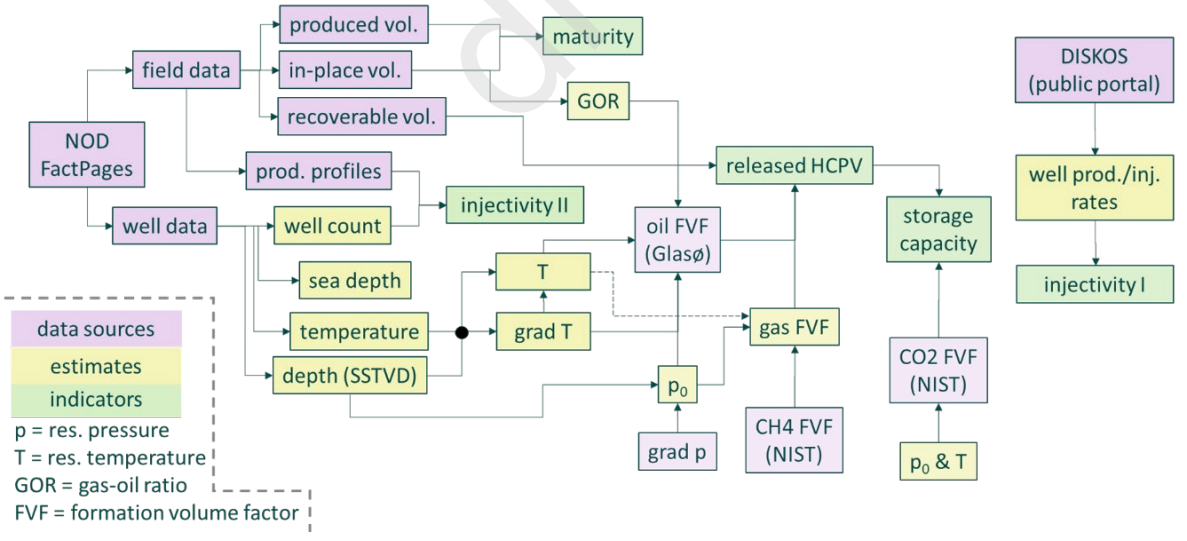

Fig. 1. Simplified scheme of data sources, data flows and derived indicators

draft

2.2. Indicators

The resulting database covers 134 Norwegian fields that have been ever approved for production. The data retrieval, processing, feature engineering workflows and many other details are documented in a Jupyter Notebook named *main.ipynb* in the GitHub repository [5].

A few simple metrics were derived to characterize the extent of reserves depletion and expected abandonment time:

- **maturity index** – the ratio of the current cumulative production to the original recoverable volume, between 0 (no production) to 1 (completely depleted) for oil, gas, liquids, and oil equivalent.
- **remaining production years** or **reserve lifetime –** the ratio of the current remaining volume to the current production of oil, gas, oil equivalent (OE), only for fields with maturity index greater than 0.75.

The **reservoir depth** was estimated for each field as the average true vertical depth of its development wells and adjusted where better data were available. Development (i.e. production, injection and observation) wells were counted, with laterals considered as separate wells.

The **initial reservoir temperature (T0)** was estimated from temperatures and depths reported for exploration wells. Despite the abundant data, applying these estimates directly to all individual reservoirs proved challenging due to missing data, outliers, and verification difficulties. Therefore, we used linear regression (Fig. 2) to estimate the temperature gradient and intercept from all data points, yielding the relationship $T(z)=32.3z+7.9$ °C, where z represents subsea true vertical depth (km). For comparison, the study [6] derived a similar relationship $T(z)=31.7z+3.4$ °C for the Sleipner CO_2 storage complex. Using the derived slope, intercept, and reservoir depths, we then calculated the reservoir temperature for individual fields. The derived correlation was validated at several known data points at different NCS regions, demonstrating reasonable accuracy. A few data points were updated with more accurate estimates found in the literature. However, the accuracy could be further improved by employing more advanced data mining techniques, which is an obvious way forward.

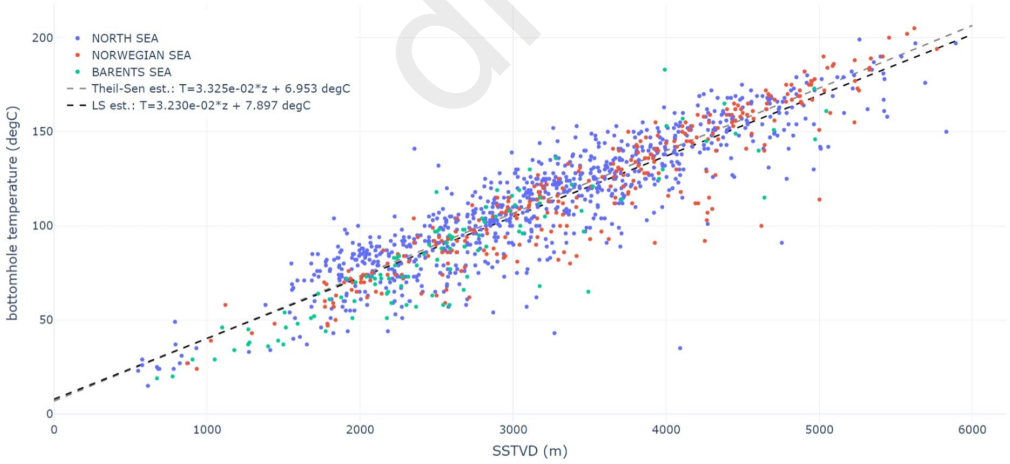

Fig. 2. Illustration of the regression of temperature data. Colors represent different NCS regions. Dashed lines depict the use of different regression methods: Theil-Sen and ordinary least squares

The **initial reservoir pressure (p0)**, in the first approximation, was assumed to be hydrostatic with a gradient of 101.8 bar/km (or 1.038 g/sm^3 in the drilling mud density equivalent). This assumption holds for most relatively shallow reservoirs (up to 2 km). However, the hydrostatic pressure gradient represents the lower boundary; and in deeper reservoirs, it may reach up to twice this value. A significant effort was made to correct pressure estimates and minimize uncertainty propagation to pressure-dependent parameters by using measurements from discovery and appraisal well reports [3], as well as regional pressure trends from [7] (e.g., for Brent reservoirs and the Greater

Ekofisk area). For more details refer to *main.ipynb* [5]. An additional property ("**p0 checked"**) was introduced to indicate whether the initial pressure was verified. The ratio of initial pressure to depth yields the **initial pressure gradient**, which, if the field is overpressured, may suggest a limited connected aquifer volume.

The **initial gas-oil ratio** (GOR) was estimated as the ratio of the associated gas volume to the Stock Tank Oil Initially in Place and corrected where possible. The gas Formation Volume Factor (FVF) was estimated for methane at the initial pressure and temperature using the NIST database [8]. Although the dry gas assumption may yield relatively large errors for wet gas reservoirs, we believe these errors to be consistent with the quality of the input data and acceptable for the purposes of this study. A similar reasoning applies to the use of the Glasø correlation to estimate the oil FVF. The CO_2 reservoir density was also calculated from the NIST data [8] at the initial pressure and temperature.

The derived parameters allow for estimating the initial hydrocarbon pore volume (HCPV) and its share released during production. By multiplying this released volume by the CO_2 density at initial pressure and temperature (calculated from the NIST data tables [8]), we obtain a **CO_2 storage capacity indicator** (similar to the metric proposed in [9]). The physical meaning of the indicator is the amount of CO_2 that can be stored in the reservoir at the initial pressure in the absence of: 1) compaction, 2) CO_2 dissolution in oil and brine, 3) water volumes injected for pressure support (mainly, due to availability and verification difficulties). The storage capacity indicator divided by the well count gives the **storage capacity per legacy well**, which can be used to factor in well leakage risk if there are such concerns.

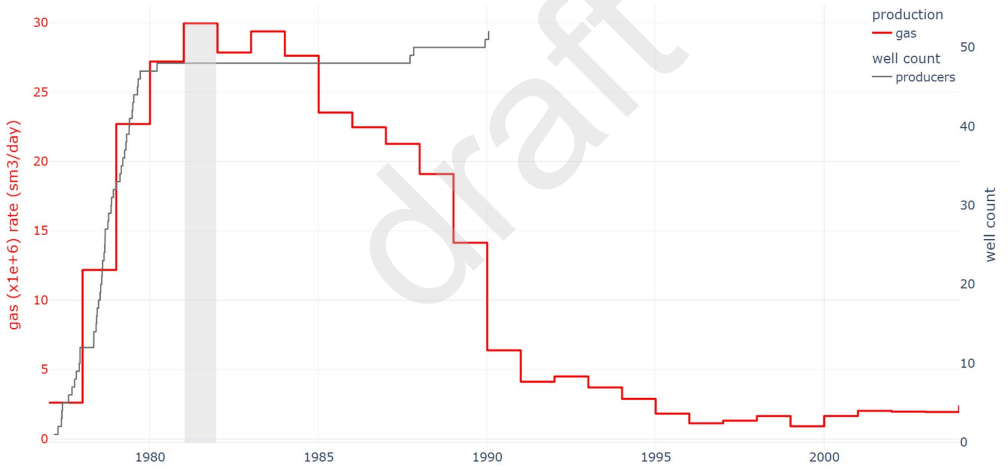

Fig. 3. Illustration to the 2nd method to calculate the injectivity indicator: gas production rate (the left y-axis) of the Frigg field and the well count (the right y-axis). The production peak year is shaded.

Injectivity indicators aim to assess the reservoir flow properties through its production history, as higher historical production/injection well rates are likely associated with better reservoir flow properties. Water/gas injection rates could potentially serve as a good benchmark; however, they are unavailable for fields produced by depletion. Moreover, gas injection is often used to utilize excessive gas volumes produced in oil fields. On the other hand, while production rates are readily available, consistent comparison between oil and gas producing wells is challenging due to differences in pressure, volume, temperature (PVT) properties, and production constraints. In our study, we addressed this challenge by converting production volumes to pseudo-reservoir conditions, using the calculated formation volume factors at initial reservoir pressure and gas-oil ratio. I.e. the physical meaning is to track how quickly the reservoir pore volume was vacated during production. Two injectivity indicators were calculated from:

1. well production data from DISKOS [4] (fluid production rates and operating time)
2. field production and well count data from NOD FactPages [3].

Both indicators were calculated for the peak production year. The second formulation (Fig. 3) can be used if production data are unavailable on a per-well basis, though it is significantly less accurate as it does not account for the well operating efficiency. The first formulation will be used throughout the remainder of this paper.

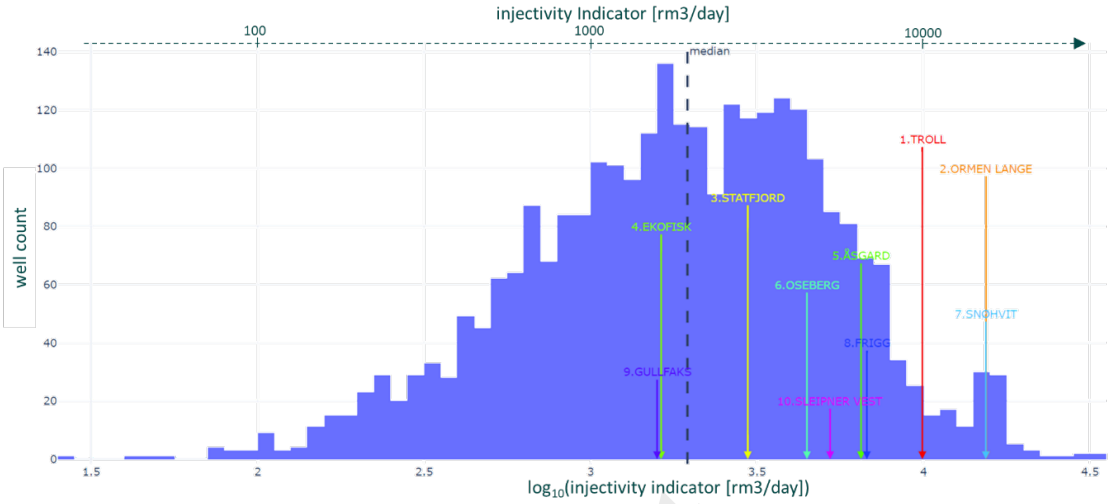

Fig. 4. Histogram of log10 (Injectivity Indicator) for all available production wells with marked top 10 reservoirs by storage capacity

Fig. 4 shows the distribution of the base-10 logarithm of the injectivity indicator for all available production wells on the NCS, with marks for the largest reservoirs by storage capacity. The gas reservoirs appear to have significantly higher injectivity indicator scores than the oil reservoirs. The correlation coefficient between the indicator and gas share of HCPV is 0.61, which can be explained by the significantly lower viscosity of gas compared to oil. The distribution appears to follow a lognormal pattern with the median around 2000 rm^3/day. At a CO_2 reservoir density of 650 kg/m^3, the median corresponds to approximately 3000 t/day or 1.12 Mt/year. However, this indicator does not account for relative permeability effects, which are likely to be significant for multi-phase flow. Although the indicator does account for viscosities of reservoir fluids and their flow properties as if they were flowing ahead of the CO_2 plume at the initial pressure and temperature. Additionally, this approach does not account for the development of drilling and completion technology; for instance, wells completed in the 1990s and later are more likely to be horizontal or multilateral, reflecting more advanced technologies and, hence, more productive. Nonetheless, we believe the approach provides reliable conservative mean estimates suitable for screening purposes.

2.3. Total score

The indicators described above and other parameters were compiled into a database that covers 134 Norwegian fields that have ever been approved for production. The indicators and other quantitative parameters can be aggregated into a **total score** – a single metric assigned to the field that characterizes its suitability for CO_2 storage. In our current implementation, the total score is calculated as a weighted average of normalized indicators as follows:

1) The user defines the parameters of interest and assigns them weights.
2) If a parameter needs to be minimized (e.g., remaining reserve lifetime before the reservoir can be converted to a CO_2 storage), it is transformed as follows:
   $x \rightarrow max(x) + min(x) - x$. This transformation is performed to keep components of the total score positive, mainly for visualization purposes. In the screening application described further, the user may hint that the parameter needs to be minimized by assigning a negative weight.
3) A **utility function** is applied to each indicator to map its nominal value to a value meaningful to the user. For instance, if the utility function of the injectivity is log_{10}, the increase from 1 to 10 sm^3/day/bar would

result in the same increment of the utility function as the increase from 10 to 100 sm^3/day/bar. This step is optional.

4) The vectors are **normalized** by one (or two compatible) of the following methods:
   a) the min-max scaling (default option) maps the parameter between 0 (worst) and 1 (best)
   b) Z-score scaling centers the data around zero mean, with the unit standard deviation.
   c) median and mean scaling center the data around 1 using median/mean value, respectively.
5) The **total score** is calculated as a weighted average of parameters based on user-defined weights. The result is multiplied by 100.

The scoring procedure and data have been implemented in a web application for visualization and screening at *https://subcset-35e143428f88.herokuapp.com/*. Illustrative case studies are provided in the next section.

3. Demonstration of the screening tool

Since 1971, 134 fields on the NCS have been approved for oil and gas production. Fig. 5 shows a map generated by the screening tool displaying all the fields with circle sizes and colors representing the storage capacity and injectivity indicators, respectively. The same figure lists the ten largest fields in terms of the storage capacity indicator, along with each field's respective maturity index. The calculated total storage capacity indicator from all fields is approximately 18 Gt, with 64% originating from the ten largest fields. Notably, the Troll field stands out significantly, accounting for approximately one-third of the total storage capacity indicator.

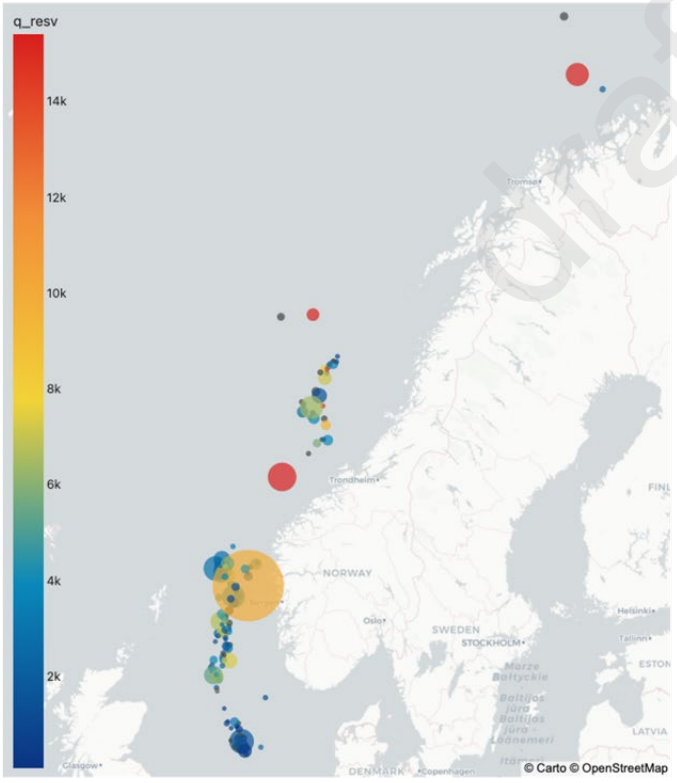

field	HC type	maturity OE	CO_2 SC indicator
		fraction	Mt
Troll	gas/oil	0.648	6.09E+03
Ormen Lange	gas	0.776	9.72E+02
Statfjord	oil/gas	0.982	7.27E+02
Ekofisk	oil	0.953	7.14E+02
Åsgard	gas/oil	0.905	6.33E+02
Oseberg	oil/gas	0.881	6.32E+02
Snøhvit	gas	0.364	6.29E+02
Frigg	gas/oil	1.000	4.12E+02
Gullfaks	oil	0.969	3.99E+02
Sleipner Vest	gas	0.955	3.96E+02

Fig. 5. Petroleum fields on the NCS, where the size represents storage capacity, the color reflects injectivity (rm3/day), and the table to the right lists the ten largest fields in terms of storage capacity, in megatonnes (Mt).

Fig. 6(a) displays a scatter plot with the storage capacity (x-axis) and injectivity (y-axis) indicators, maturity index (color), and initial reserves in oil equivalent (size) of all the fields (with the two largest fields named). Fig. 6(b)

displays a scatter plot with the depth (x-axis), CO_2 density in reservoir conditions (y-axis), initial pressure gradient (color), and storage capacity indicator (size). Several fields are named in the figure, and, for illustration purposes, Troll (with the largest storage capacity indicator) is excluded from this plot. Notably, the CO_2 density remains nearly constant at approximately 650 kg/m³ in fields under the hydrostatic conditions (depicted in dark blue, forming the straight line along the chart's bottom), almost independent of depth, as the hydrostatic pressure and temperature gradients' effects offset each other.

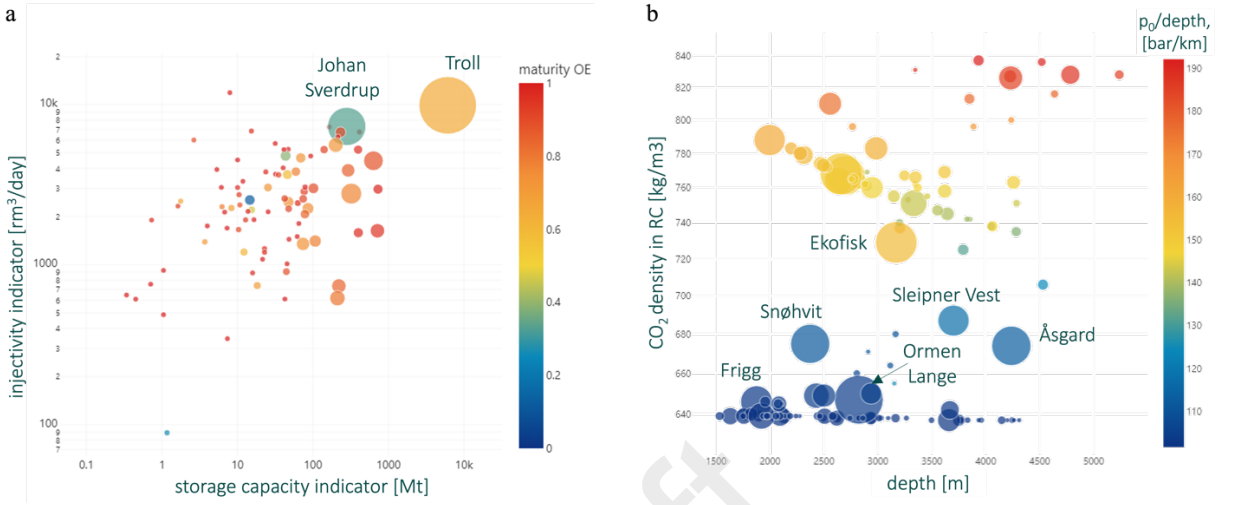

Fig. 6. (a) all fields visualized by size (initial reserves in oil equivalent), color (maturity index) and injectivity indicator (rm3/day); (b) all fields (except Troll) visualized by size (storage capacity indicator), by color (initial pressure gradient).

3.1. Case 1: Storing CO_2 close to available CCS infrastructure.

The first case illustrates how the screening tool can be used to evaluate storage candidates near available infrastructure. The ongoing Norwegian "Longship" full-scale CCS project will soon start injecting CO_2 in the Aurora area, in exploitation license EL001, southwest of the Troll field [10,11]. The project's onshore facility in Øygarden (Western Norway) will serve as the receiving terminal for CO_2, which will be transported by pipeline to the Aurora offshore storage site. This area is particularly interesting because Aurora is bordered by the Smeaheia storage exploration license (ExL002) to the east and by the Luna exploration license (ExL004) to the west. Nine producing and two decommissioned fields can be found in immediate proximity to these licenses (Fig. 7).

draft

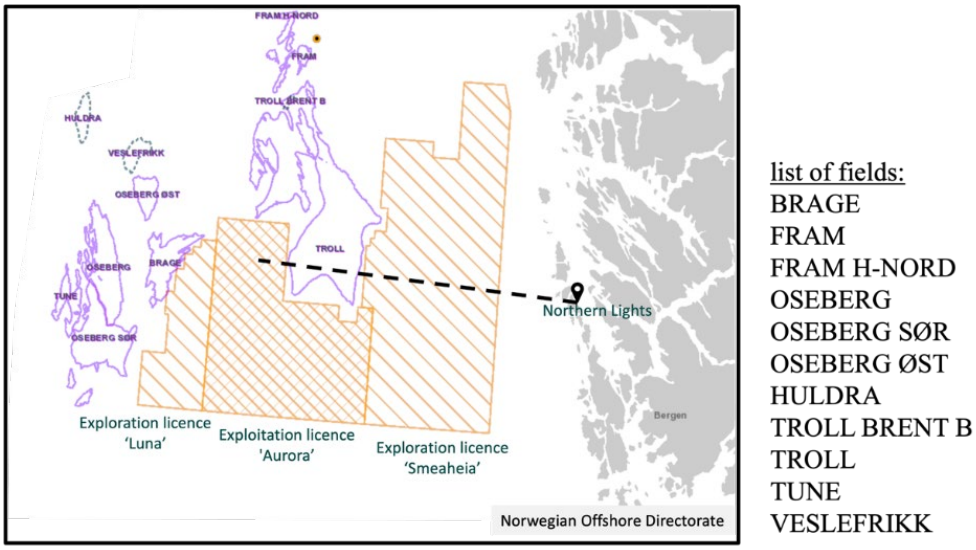

Fig. 7. Petroleum fields east and north of the Luna, Aurora, and Smeaheia licenses west of the Northern Lights onshore facilities in the Western Norway, the map is generated at FactMaps by Norwegian Offshore Directorate (https://factmaps.sodir.no/factmaps).

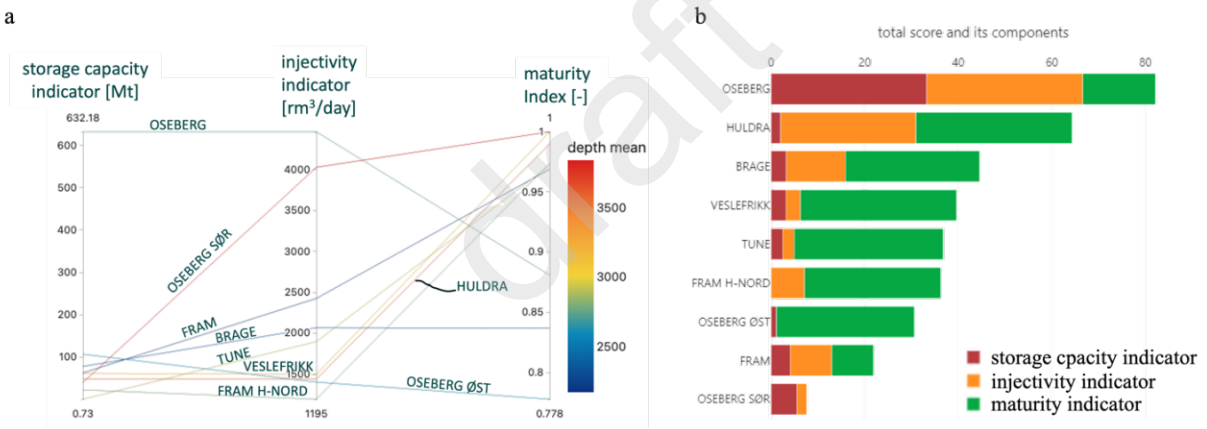

Fig. 8. (a) Parallel plot of the depth, storage capacity indicator, injectivity indicator, and maturity index for the selected fields generated by the screening tool; (b) Total score for the selected fields based on equal weights for storage capacity indicator, injectivity index, and maturity indicators.

After excluding the giant gas fields Troll and Troll Brent B, the remaining nine fields are evaluated by the above-described indicators for capacity, injectivity, maturity, and depth displayed in Fig. 8(a). The storage capacity, injectivity, and maturity indicators are selected to calculate the total score. These metrics are assigned equal weights and normalized using the min-max scaling. As described in the previous section, both screening parameters, their weights, and the normalization method are set by the user. Based on ranking by the total score in Fig. 8(b), we conclude that Oseberg is the best candidate among the selected fields. This field has high storage capacity, injectivity and is relatively mature. However, the field does not achieve the highest scores for all criteria, as its total score, calculated using min-max scaling, falls below 100.

3.2. Case 2: Storing CO_2 from a large emitter from petroleum activities nearby

Over the last 26 years, the Ekofisk field has been one of the largest emitters of CO_2 on the NCS, with an average emission of 0.76 Mt per year (0.53 Mt in 2023) [12]. In its vicinity, there are 14 mature and abandoned petroleum fields that reached their peak production before 2013. Fig. 9 presents a map with these fields, where the size of each circle represents the storage capacity indicator (with Ekofisk displayed as the largest circle). Fig. 10(a) shows the storage capacity indicator, injectivity indicator, remaining reserves, depth and initial pressure gradient for these fields. Fig. 10(b) shows the fields ranked by the resulting total scores calculated with equal weights for the storage capacity, injectivity and maturity indicators. In the described scenario, based on the total score, Ula, Vest Ekofisk and Tommeliten Gamma are the best candidates to store CO_2 from Ekofisk. However, again, none of the fields is the best by all the criteria, as the highest total score, calculated using min-max scaling, falls below 100.

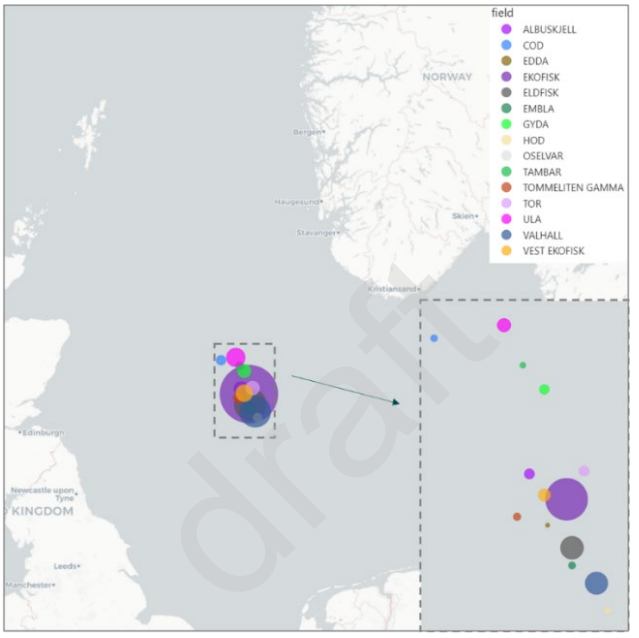

Fig. 9. Ekofisk and 14 mature or shut down petroleum fields located nearby. The circle sizes reflect the storage capacity indicator.

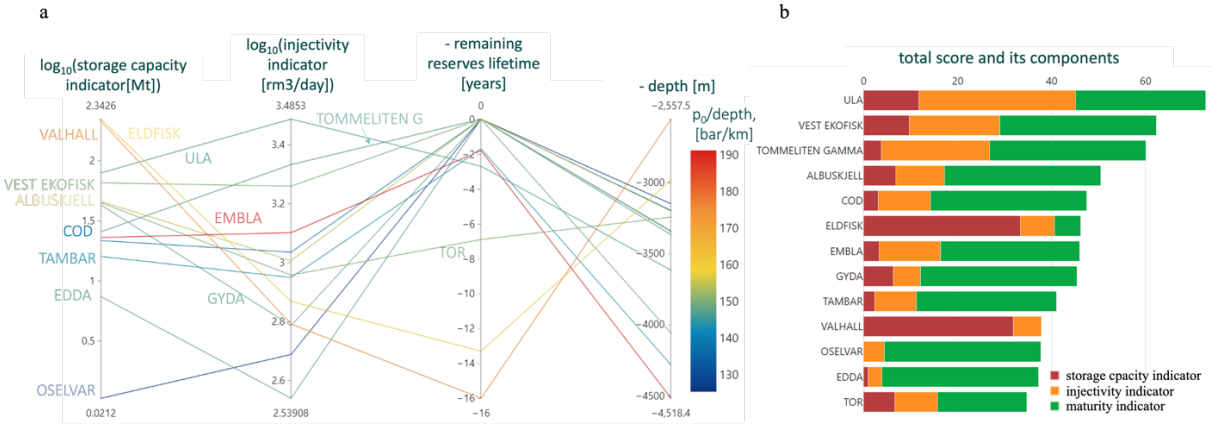

Fig. 10. (a) parallel plot with data for the selected neighboring fields of Ekofisk; (b) total score for these fields applying an equal weight on the storage capacity indicator, the injectivity indicator and the maturity indicator.

4. Discussion

We believe that the current study creates value by gathering, processing, enriching and analyzing public data, and redistributing the results back to the public domain. There remains considerable potential for further work in any of these directions. The presented approach could be enhanced with more available data and provide a better and more nuanced assessment.

As briefly discussed above, the proposed approach is limited by the data resolution and assumptions made to bridge missing data. In particular, this study was performed in quasi-2D, as the data were aggregated on the field level and did not allow for discerning separate formations within a given field.

Above, while introducing the indicators, we have already touched upon some of their limitations. The **storage capacity indicator** does not account for compaction, communication with adjacent aquifers, and water volumes injected for pressure support. Nor does this indicator account for sweep, displacement, and drainage efficiency factors of CO_2 storage, which are the subjects of detailed studies. We believe that integration of dynamic pressure measurements would allow for delineating compaction effects and aquifer communication. The same applies to water volumes injected. In the current study, we did not manage to integrate injected water volumes due to data availability and verification difficulties, though it would greatly enhance estimates for oil fields produced under waterflooding. The reduction of available pore volume due to water injection will decrease the storage capacity estimates, especially in confined reservoirs. However, this impact is not likely to be very significant for the total storage capacity as its bulk (69%) is associated with pore volumes released in gas fields, which are normally depleted without pressure support. Moreover, the current formulation of the storage capacity indicator does not account for possible upsides due to 1) additional capacity associated with adjacent aquifers and 2) pressurization above the initial pressure. The latter can be addressed by integrating fracturing pressure estimates from leak-off tests [14,15].

In general, we are cautious about equating the storage capacity indicator with a bankable storage capacity, as the former has the limitations mentioned above, while the latter is subject to certain methodological vagueness that can hardly be resolved without detailed, case-by-case studies. Overall, the indicator falls into the category of static storage capacity estimates, which may significantly exceed commercial capacity. As hydrocarbons are trapped within deposits covered by caprocks, injected CO_2 is unlikely to migrate upwards, provided that there is no leakage through legacy wells or severe fracturing. Therefore, we believe that, in the first approximation, the entire released HCPV can be claimed for CO_2 storage.

During CO_2 injection, three flow regions emerge: 1) CO_2 around the well, 2) CO_2 mixed with original fluids (brine, oil, gas), and 3) original fluids displaced away from the well by the CO_2 plume. The proposed **injectivity indicator** is based on production data and, hence, the most suitable to describe the third region. It reflects the flowing properties of original fluids, but does not account for CO_2 and multiphase flow in the first and second regions. The injectivity indicator formulation could further be refined, for instance, through simple analytical models for solvent flooding and/or numerical modeling. Above, it was demonstrated (Fig. 4) that the injectivity indicators of individual wells on the NCS follow a pseudo-lognormal distribution, which may reflect fundamental laws governing the distribution of flow properties, such as permeability. At the field level, the distribution of historical well rates can be utilized to characterize heterogeneity and assess the uncertainty associated with injectivity.

A simplistic formulation used for the **reserve lifetime** is not very accurate and does not apply to green fields. It is possible to develop a more advanced, data-driven formulation that leverages the typical growth-decline dynamic of petroleum production, thereby enhancing accuracy. Additionally, introducing an **energy efficiency indicator** would allow for ranking reservoirs by specific energy per CO_2 unit stored.

5. Summary and conclusions

This study utilized publicly available data about almost all Norwegian petroleum fields to assess their CO_2 storage potential through indicators for essential parameters such as storage capacity, injectivity, etc. The total storage capacity indicator for the NCS was estimated at 18 Gt, with 64% attributed to the ten largest fields and 69% to gas production. The proposed methodology is not intended to provide a comprehensive analysis; however, it can still narrow the list of available options, answer essential questions, highlight knowledge gaps to be addressed in detailed studies, and consistently rank candidate reservoirs. Additionally, the findings and data from this study can be applied to other purposes, such as hydrogen storage. There is a significant potential for further reuse of data from petroleum reservoirs.

The repository with the data and codes is available at *https://github.com/cssr-tools/SubCSeT*. A web application for data visualization and screening can be accessed at *https://subcset-35e143428f88.herokuapp.com/.*

6. Acknowledgement

The authors acknowledge funding from the Centre of Sustainable Subsurface Resources (CSSR), grant nr. 331841, supported by the Research Council of Norway, research partners NORCE Norwegian Research Centre and the University of Bergen, and user partners Equinor ASA, Harbour Energy Norge AS, Sumitomo Corporation, Earth Science Analytics, GCE Ocean Technology, and SLB Scandinavia.

Nomenclature

FVF	formation volume factor (rm^3/sm^3)
GOR	gas-oil ratio (sm^3/sm^3)
HCPV	hydrocarbon pore volume (rm^3)
NCS	Norwegian Continental Shelf
OE	oil equivalent (1 sm^3 of oil or 1000 sm^3 of natural gas)
PVT	pressure volume temperature (fluid properties)
STOIIP	Stock Tank Oil Initially in Place (sm^3)
SSTVD	subsea true vertical depth (m)

draft

References

[1] Norwegian Offshore Directorate. Resource report 2024 [Internet], 2024, Available from: https://www.sodir.no/en/whats-new/publications/reports/resource-report/resource-report-2024/
[2] U.S. Department of Transportation. Fact Sheet: Underground Natural Gas Storage Caverns | PHMSA [Internet]. 2021, Available from: https://www.phmsa.dot.gov/technical-resources/pipeline/underground-natural-gas-storage/fact-sheet-underground-natural-gas
[3] FactPages. Norwegian Offshore Directorate [Internet], Available from: https://factpages.sodir.no/
[4] DISKOS database. Public production [Internet], Available from: www.diskos.com
[5] Khrulenko A. SubCSeT project repository [Internet], Available from: https://github.com/cssr-tools/SubCSeT
[6] Alnes H., Eiken O., Nooner S., Sasagawa G., Stenvold T., Zumberge M. Results from Sleipner gravity monitoring: Updated density and temperature distribution of the CO2 plume. Energy Procedia. 2011;4:5504–11.
[7] Moss B., Barson D., Rakhit K., Dennis H., Swarbrick R. Formation pore pressures and formation waters. In: The Millennium Atlas: petroleum geology of the central and northern North Sea. Evans, D, Graham, C, Armour, A, and Bathurst, P (editors and co-ordinators). London: The Geological Society of London.; 2003. p. 317–29.
[8] Lemmon E.W., Bell I.H., Huber M.L., McLinden M.O.. Thermophysical Properties of Fluid Systems in NIST Chemistry WebBook. NIST Standard Reference Database Number 69, Eds. P.J. Linstrom and W.G. Mallard, National Institute of Standards and Technology, Gaithersburg MD, 20899, [Internet]. Available from: https://doi.org/10.18434/T4D303
[9] Ramírez A., Hagedoorn S., Kramers L., Wildenborg T., Hendriks C. Screening CO2 storage options in The Netherlands. International Journal of Greenhouse Gas Control. 2010 Mar;4(2):367–80.
[10] Ministry of Petroleum and Energy. Longship – Carbon capture and storage — Meld. St. 33 (2019–2020) Report to the Storting (white paper) [Internet]. 2020. Available from: https://www.regjeringen.no/en/dokumenter/meld.-st.-33-20192020/id2765361/

[11] Equinor. Northern Lights FEED report [Internet]. Available from: https://norlights.com/wp-content/uploads/2021/03/Northern-Lights-FEED-report-public-version.pdf
[12] The Norwegian Environment Agency. Ekofisk: Releases of Carbon dioxide (CO2) [Internet]. Available from: https://www.norskeutslipp.no/en/Miscellaneous/Company/?CompanyID=22344&ComponentPageID=1162
[13] Gaarenstroom L., Tromp R.A.J., De Jong M.C., Brandenburg A.M. Overpressures in the Central North Sea: implications for trap integrity and drilling safety. PGC. 1993 Jan;4(1):1305–13.
[14] Nordgård Bolås H.M., Hermanrud C. Hydrocarbon leakage processes and trap retention capacities offshore Norway. PG. 2003 Oct;9(4):321–32.

draft